Nanomed Res J 8(1): 94-101, Winter 2023

RESEARCH ARTICLE

Assessing the cytotoxic functionality of Co-CeO2 nanoparticles towards colon cancer and mouse embryo fibroblast cells

Mohammed Mahdi Nemati[1], Mohammad Mahdi Tanidehvar[2], Elahe Derakhshan[3], Pooya Jafari Doudaran[4,5], Bahareh Mahdood[6], Minoo Roostaie[7*]

[1]Faculty of Medicine, Urmia University of Medical Sciences, Urmia, Iran.
[2]Faculty of Basic Sciences, Islamic Azad University, Science and Research Branch, Tehran, Iran.
[3]Department of Biotechnology, Faculty of Chemical Engineering, Tarbiat Modares University, Tehran, Iran.
[4]Student research committee, Qom University of Medical Sciences, Qom, Iran
[5]Department of Nursing Qaenat Branch, Islamic Azad University, Qaenat, Iran
[6] Department of Operating Room, Faculty Member of Paramedical School, Jahrom University of Medical Sciences, Jahrom, Iran
[7] School of Medicine, Islamic Azad University, Tehran Medical Branch, Tehran, Iran.

ARTICLE INFO

Article History:
Received 25 Nov 2022
Accepted 14 Dec 2022
Published 15 Feb 2023

Keywords:
Co-CeO2 NP
Raman
MTT Assay
Colon Cancer

ABSTRACT

Nowadays, development and currency of cancer led to the conduction of many attempts for finding novel compounds with the ability to subdue a tumor while causing a lower rate of toxicity. The numerous applications of metal oxide nanoparticles in biology and biomedicine are the result of their distinct physical and chemical features. In this regard, we attempted to introduce an uncomplicated, easy, and green approach to produce of pure and 5% cobalt doped cerium oxide nanoparticles (Co-CeO_2 NP) through the exertion of *Biebersteinia multifidi* leaf extract in the form of a proposed compound for cancer treatment. The finding of performed PXRD, FESEM, EDX, and Raman procedures conFig.d the morphology and size of cobalt doped cerium oxide to be spherical along with a size about 10 nm Additionally, MTT assay was implicated to investigate the toxicity impact of synthesized pure and Co-CeO_2 NP against colon cancer (CaCo2), and mouse embryo fibroblast (NIH-3T3) cell lines. Accordingly, the non-toxicity of cerium oxide nanoparticles towards cancer and normal cell lines were proved, whereas the Co-CeO_2 NP exhibited cytotoxic effects on CaCo2 cell line while the NIH-3T3 cell line was an exception in comparison to doxorubicin as the control. Considering these facts, the adequate inhibitory impact of synthesized Co-CeO_2 NP on colon cancer cell line can be affirmed.

How to cite this article
Nemati M. M., Tanidehvar M. M., Derakhshan E., Jafari Doudaran P., Mahdood B., Roostaie M., Assessing the cytotoxic functionality of Co-CeO2 nanoparticles towards colon cancer and mouse embryo fibroblast cells. Nanomed Res J, 2023; 8(1): 94-101. DOI: 10.22034/nmrj.2023.01.009

INTRODUCTION

In the form of a springing technology, nanotechnology implicates the design of structures in nano size to provide an uncountable amount of innovative and useful features, which has been also reported in the work of numerous researchers around the world [1-4] . Cerium oxide nanoparticles are known to be consisted of cerium atoms that are encircled by oxygen networks. This product is extensively employed for certain applications such as polish of mechanical chemical, solar cells, corrosion protection, and automobile exhaust treatment[5] .

Despite the fact that a small number of assessments reported the in vitro and in vivo inducement of oxidative stress, the explicit functionality of nanoceria as an antioxidant and its activity in the form of a free radical scavenger is undeniable [5-7]. Therefore, the suitability of CeO_2 NP for being applied as potential drug agents in pharmacy applications and biological scaffolding

* Corresponding Author Email: *minooroosta@gmail.com*

can be affirmed [8-11]. There used to be an initial belief that supposed the implication of both oxygen vacancy and redox cycles between these two cerium states in antioxidant activities, however, recent discoveries confirmed the fundamental accountability of redox cycles to all antioxidant features[12, 13]; while the surface ratio of Ce^{+3}/Ce^{+4} has a major functionality in most of the biological applications of CeO_2 NP [14] . Considering their further abilities in acting as oxidants at low pH and high doses, CeO_2 NP can exhibit cytotoxic effects through the appropriate synthesizing procedure, volume, and duration of exposure[15] . In this regard, the production of relatively non-toxic CeO_2 NP with oxidant or antioxidant features can be achieved by facilitating a careful optimization over suitable synthetic parameters[5].

The kind of exerted synthesizing procedure is the main determining factor for the obtained physic-chemical features of nanoparticles, which arose the idea of prospecting the production of CeO_2 NP with varying sizes, morphology, and accumulation. The recent engrossment towards bio-inspired biological routes that are applied in the form of stabilizing agents throughout the generation of CeO_2 NP is due to the decreased concerns in terms of biocompatibility. Complying with the standards [16] of green chemistry resulted in the facilitation of safer production methods for this product that can be practical for drug implementations. It is also noteworthy to consider their affordable costs and more manageable options when compared to that of traditional chemical synthesizing procedures [17-21]. The achievement of efficient and essential nanoparticles qualities also relies on the fundamental parameter of doping process. According to the confinement of several reports, there were conspicuous modifications observed in the features of nanoparticles that were doped with various metals when compared to that of un-doped nanoparticles, whereas the doped products were procured through similar synthesizing routes [22-24].

As a perennial herbaceous plant, *Biebersteinia multifida* is consisted of thick roots and stems along with a large number of longitudinal grooves that contain a covering of tuberous protrusions, which grows in several forms with varying alkaloids throughout Iran, Lebanon, Armenia, Syria, and Afghanistan [25] .In this project, we conducted the synthesis of pure and cobalt doped cerium oxide nanoparticles through the implication of *B. multifida* leaf extract to evaluate the cytotoxicity of obtained product on colon cancer (CaCo2) and mouse embryo fibroblast (NIH-3T3) cell lines**.**

MARTIAL AND METHODS

Prepare of pure and Co-CeO_2 NP

In order to deploy the extraction of *B. multifidi* for the synthesizing process, the leaf of *B. multifidi* was cleaned to be dried and crushed. Then, 100 mL of distilled water (1:10 ratio) was used for dissolving 10 gr of plant powder under shaking conditions at 150 rpm for 24 hours. Subsequent to filtering the mixture through a Whatman 1 filter paper, it was required to dilute 10 mL of the extract with 50 mL of distilled water. Once 50 mL of $Ce(NO_3)_3.6H_2O$ (0.02 M) and $Co(SO_4).7H_2O$ (in ratios of 0 and 5 w/w, separately) was appended to the extract solution, the mixture was put in a water bath at the temperature of 70 °C for 3 hours. Next to the centrifugation step, we dried the solutions by an oven (90 °C) to calcine the procured residue through a digital furnace at 400 °C for 2 hours.

Characterization

Powder X-ray diffraction (PXRD) spectra of the generated nanoparticles were provided by the exertion of X-ray diffraction model X'Pert PRO MPD PANalytical Company (Netherlands Formation). Furthermore, scanning electron microscopy (SEM), TESCAN model MIRA3 was considered for identifying the obtained morphology, while the achievement of Raman spectra required the deployment of a Raman Takram P50C0R10 at the wavelength of 532 nm.

Cytotoxic activity

Cell culture

The cell lines of CaCo2 and NIH-3T3 cells were acquired from the Iranian Biological Resource Center (IBRC, Tehran, Iran). In the following, we used separate 96 multi-well plates to seed the cells at a density of 10×10^3 cells per well at the temperature of 37 °C for 24 h for obtaining confluences. Then, involved the treatment of cells with different volumes of nanoparticles (1–1000 µg/mL) for the duration of 24 hours, while doxorubicin was exerted in the form of a positive control. Once 10 µL of MTT reagent was applied to every well, an incubation process was performed for another 4 h at the temperature of 37 °C in dark. Subsequent to the dispatching of medium, we appended 100 µL of DMSO into every well and exerted a

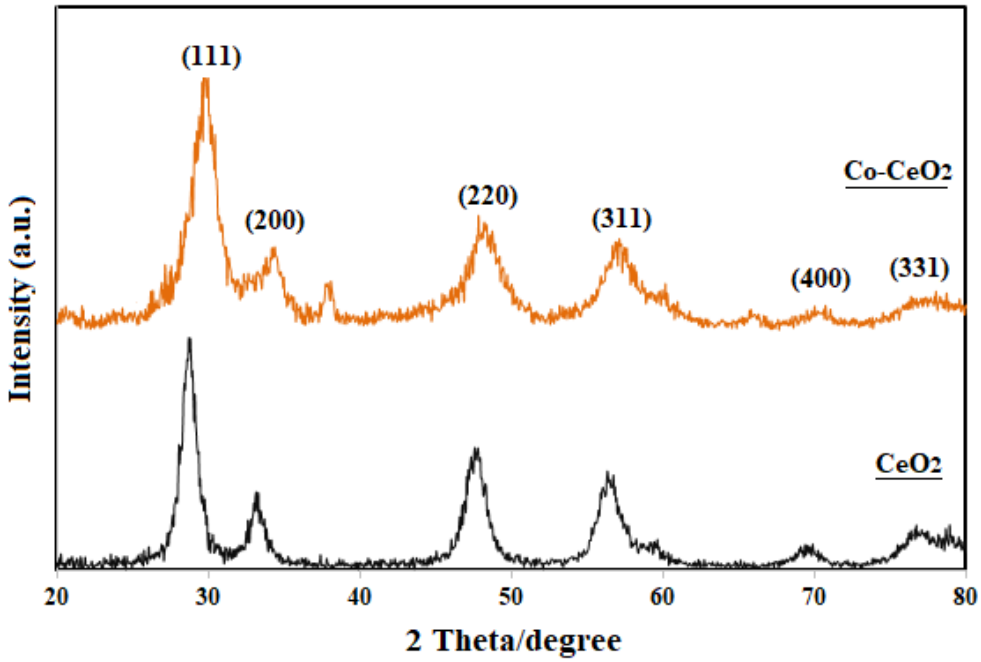

Fig. 1. PXRD spectra of pure and 5% Co-CeO_2 NP using *B. multifidi* leaf extract

microplate reader to record generated formazan by determining the absorbance at the wavelength of 570 nm. The viable cell percentages were exhibited in regards to the vehicle-treated group.

MTT assay

Separate 96 multi-well plates were utilized at a density of 10×10^3 cells per well for the seeding process of **c**ell lines (CaCo2, and NIH-3T3) at the temperature of 37 °C and the duration of 24 h for confluence purposes. In the course of cells treatment with varying volumes of nanoparticle (1–1000 µg/mL) for 24 hours, Doxorubicin acted as the positive control. As the next step, we appended 10 µL of MTT reagent to every well to perform incubation for another 4 h at 37 °C in dark. Subsequent to the dispatching of medium, the addition of 100 µL of DMSO was considered for every well and thereafter, the exertion of a microplate reader helped in recording the generated formazan by reading the absorbance at the wavelength of 570 nm. The viable cell percentages were exhibited in regards to the vehicle-treated group.

RESULTS AND DISCUSSION

XRD analysis

Fig. 1 demonstrates the XRD spectra of pure and 5% Co-CeO_2 NP for configuring the crystalline features of synthesized products. The appearance of peaks can be observed throughout the areas of 28.74, 33.16, 47.72, 56.53, 69.49, and 76.91° that were in accordance to (111), (200), (220), (311), (400), and (331) levels, which signified the existence of a face-centered cubic (FCC) construction (JCPDS: 00-043-1002). A mild alteration in (111) peak was detected subsequent to the doping of Co into CeO_2 structure, which confirms the successful entry of doped materials. This observation could be associated with the dissimilar ionic radii of Co and Ce atoms, since the ionic radius of $Co^{+2/+3}$ (0.75-0.9 Å) is lower than that of Ce^{+4} (0.97 Å). In conformity to Fig. 1, an expansion was induced in the peaks as a result of extending the percentage of doped Co, which may be attributed to the reduced particle size (Fig. 1). The Debye-Scherrer [19] equation was applied to the data of PXRD spectra to estimate the crystalline size of pure and 5% Co-CeO_2 NP to be 9.24 and 7.02 nm, respectively; apparently, the doping of cobalt stood responsible for the decreased crystalline size of synthesized products.

FESEM and EDX analysis

A precise comprehension on the shape and size NP was provided by the outcomes of FESEM imaging for the cases of pure and 5% Co-CeO_2 NP, which is presented in Fig. 2. Although the size of CeO_2 NP was initially less than 10 nm, yet it became even smaller subsequent to the doping

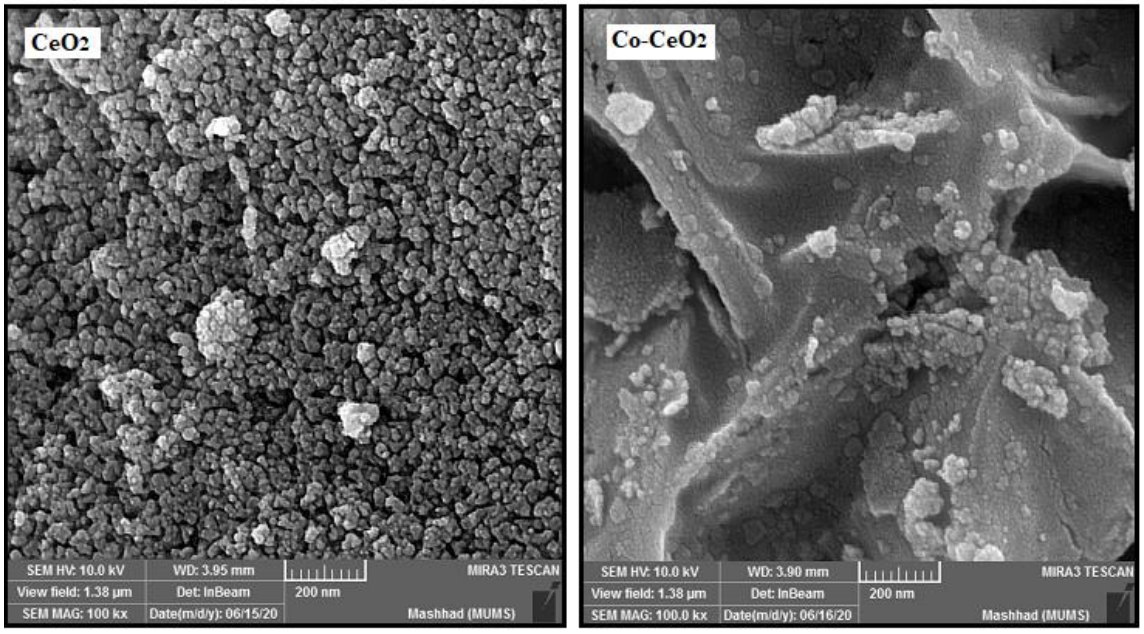

Fig. 2. FESEM images of pure and 5% Co-CeO_2 NP using *B. multifidi* leaf extract

process of cobalt. Considering the atomic radius of cobalt (125 pm) and cerium (181.5 pm), it is presumable that escalating the applied volume of doped cobalt into the crystal construction of cerium oxide particles may cause a reduction in their sizes. The EDX images of synthesized products (Fig. 3) approved the purity and obvious entry of cobalt to the construction of cerium oxide. The percentages of Ce atom were detected to be 74.56% while the results of Co atom were 4.71%, throughout the cases of 5% Co-CeO_2 NP.

Raman analysis

In conformity to Fig. 4, the F2g state of cube fluoride construction of CeO_2 was signified by the detected band in region 459 cm^{-1}, which may be allocated to the state of Ce-O8 symmetric vibration. The reliance of vibrational state on the mass of cation is caused by the individual motion of oxygen atoms. Meanwhile, this particular band was detected in the regions of 445 cm^{-1} throughout the cases of doped CeO_2 NP with 5% cobalt. According to viable proofs, the transfer of this band to lower regions can be facilitated by intensifying the applied volume of doped Co into CeO_2. This phenomenon is induced by the creation of oxygen deficiency due to the entry of cobalt cation into the crystal construction of CeO_2 [23, 26].Moreover, since the posture of this band can be also affected by the parameter of particle size, the F2g mode was observed to be conveyed toward lower regions as a result of the reduced particle size [23].

Cytotoxic performance

We performed an investigation on cell proliferation and cell viability through the addition of tetrazolium salts to the cell culture medium, which were transformed into formazan by cellular enzymes. The functionality of mitochondrial dehydrogenase enzymes throughout the sample provided a basis for estimating the number of viable cells. Meanwhile, their higher activity is indicative of an increase in the rate of produced formazan dye within the culture medium, which is a straight sign for the amount of existing metabolically active cells. The absorbance of formazan dye solution by an ELISA reader at the suitable wavelengths can configure. the number of active cells throughout the culture medium [18].

The presented outcomes of MTT test in Fig. 5 were exerted to assess the induced cytotoxicity on colon cancer cells (CaCo2), and mouse embryo fibroblast cell (NIH-3T3) line subsequent to the application of pure and 5% cobalt doped nanoparticles. The obtained IC_{50} of synthesized products and doxorubicin as the control is demonstrated in Table 1, while Fig. 6 exhibits the cell images in prior and after being treated with 5% Co-CeO_2 NP in opposition to CaCo2 and NIH-3T3 cells.

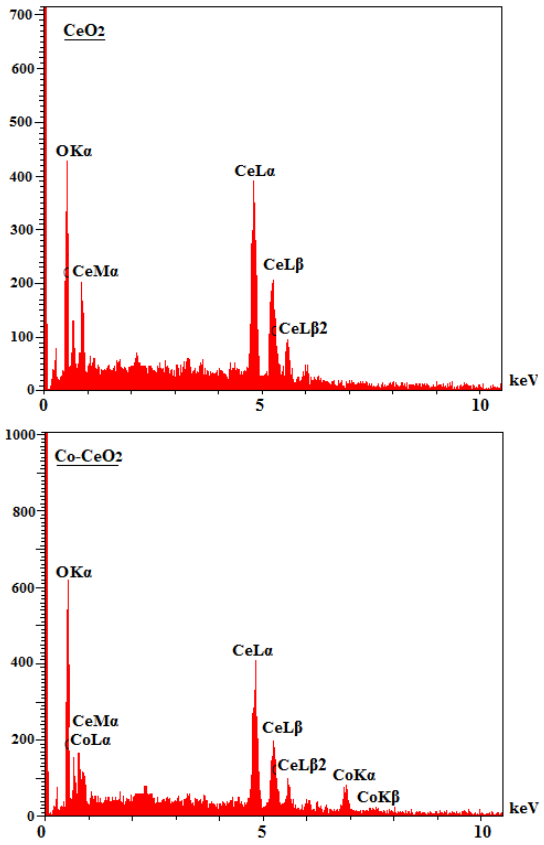

Fig. 3. EDX spectra of pure and 5% Co-CeO_2 NP using *B. multifidi* leaf extract

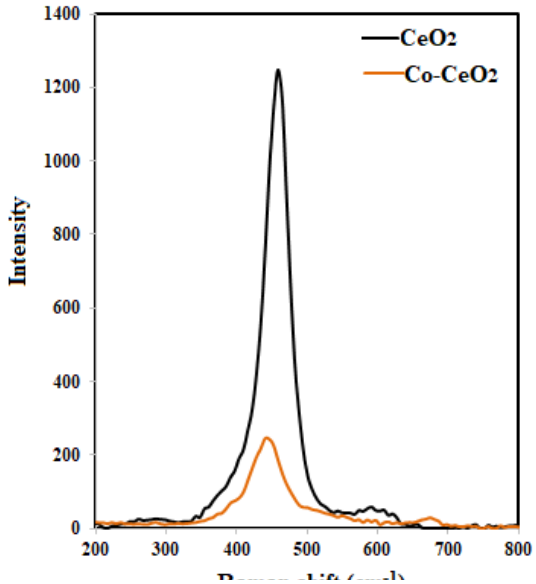

Fig. 4. Raman spectra of pure and 5% Co-CeO_2 NP using *B. multifidi* leaf extract

Table 1. IC_{50} values of pure and Co-CeO_2 NP using *B. multifidi* leaf extract

Cell line	IC_{50} of synthesized NP (µg/mL)		Control
	pure	5% doped Co	Doxorubicin
CaCo2	1172	171.2	110.1
NIH-3T3	2140	11640	759

Although the data of Fig. 6 clearly displays the non-toxicity of CeO_2 NP towards CaCo2 cell line, however, the cobalt doping process resulted in empowering the cytotoxic impacts on colon cancer cell line. The case of 5% Co-CeO_2 NP contained an IC_{50} value of 171.2 µg/mL for CaCo2 cell line, respectively, which seemed to be more parallel to the IC_{50} of doxorubicin as the control (Table 1). Nevertheless, there were no signs of any notable cytotoxicity by the doped nanoparticles throughout the NIH-3T3 cell line. It is noteworthy to mention that the application of CeO_2 NP in high volumes (≤1000 µg/mL) leads to the induction of diminutive cytotoxic impacts. The results of this work exhibited the biocompatibility of green synthesized nanoparticles, which was in agreement with previous investigations on different nanoparticles. Green synthesized biogenetic products can function as an applicable substitute with a dependency on organic organisms for reducing metal ions into stable and biocompatible NP [27-29]. For Instance, Irshad *et al.* reported the arrangement of CeO_2 NP by the exertion of orange peel extract (OPE) that succeeded in exhibiting *extraordinary* antioxidant functionality [30]. Moreover, a performed assessment by Rajan et al. implicated the utilization of Morus nigra fruit extract for fabricating CeO_2 NP to examine the obtained cell viability on L929 cell lines; their results confirmed the biocompatible behavior of this product[31] .

CONCLUSION

This work reports the results of a success attempt for arranging pure and 5% cobalt-doped cerium oxide nanoparticles by the exertion of *Biebersteinia multifidi* leaf extract. In the following, we assessed the physicochemical qualities of our product and the analytical outcomes confirmed their spherical shape and uniformity. Although the size of CeO_2 NP was less than 10 nm, yet it became even smaller as a result of doping cobalt into the construction of nanoparticles. We considered the implication of MTT assay to evaluate the

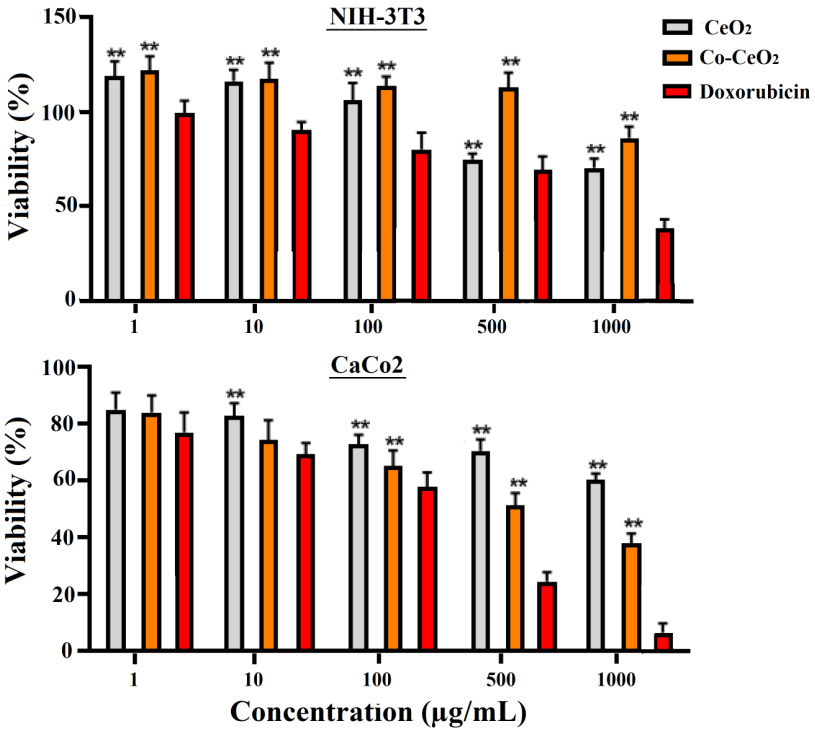

Fig. 5. Cell viability of pure and 5% Co-CeO_2 NP on CaCo2 and NIH-3T3 cell lines after 24 h incubation

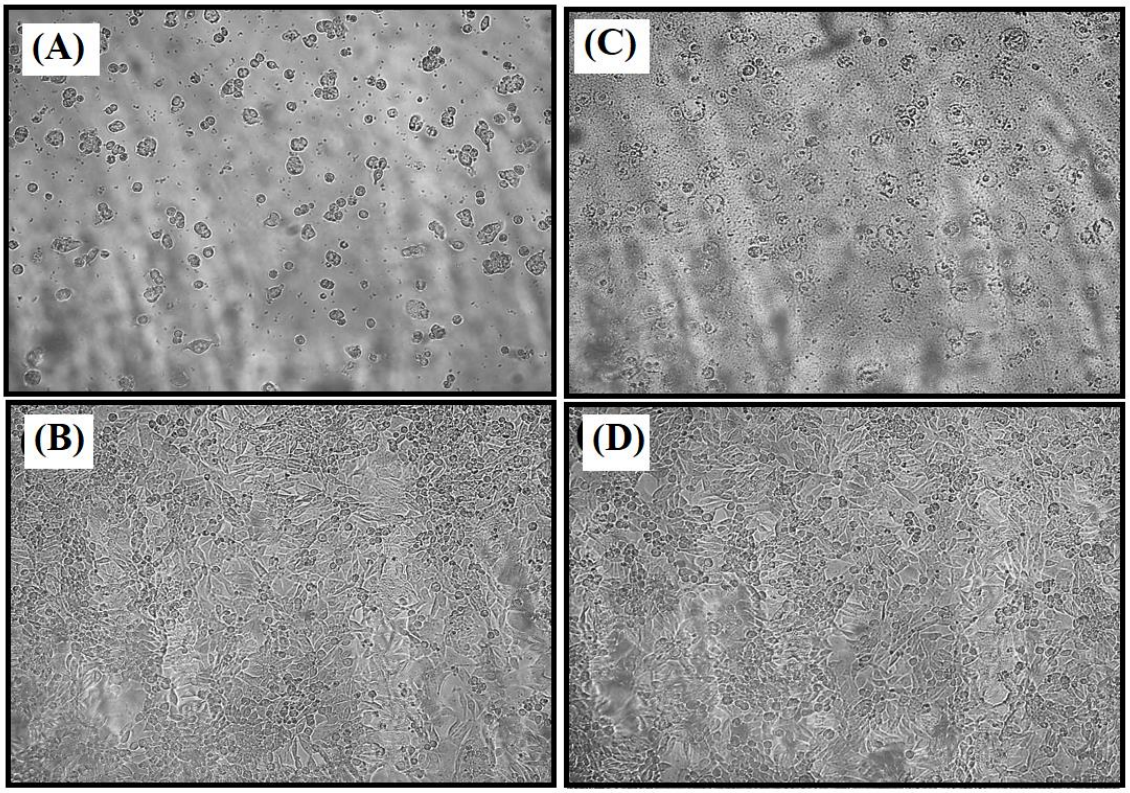

Fig. 6. Cell images (A) un-treated CaCo2, (B) un-treated NIH-3T3, (C) treated CaCo2, and (D) treated NIH-3T3 with 5% Co-CeO_2 NP.

toxicity of NP against CaCo2 and NIH-3T3 cells, which approved the non-toxicity of cerium oxide nanoparticles in all the three cell lines, while Co-CeO_2 NP exhibited some toxic attitude towards CaCo2 cell. Furthermore, observations indicated the inducement of an escalation in cytotoxicity throughout the cells as a result of expanding the percentage of applied cobalt into the construction of CeO_2. Therefore, the superior viability and applicability of our synthesized product, when compared to other formulations, can be approved for cancer treatment and associated biological implementations similar to drug delivery.

CONFLICT OF INTEREST

The authors declare no conflict of interest.

REFERENCE

1. Iravani, S. and R.S. Varma, Green synthesis, biomedical and biotechnological applications of carbon and graphene quantum dots. A review. Environmental chemistry letters, 2020. 18(3): p. 703-727. https://doi.org/10.1007/s10311-020-00984-0
2. Nadeem, M., et al., Green synthesis of cerium oxide nanoparticles (CeO2 NPs) and their antimicrobial applications: a review. International Journal of Nanomedicine, 2020. 15: p. 5951. https://doi.org/10.2147/IJN.S255784
3. Sarani, M., et al., Study of in vitro cytotoxic performance of biosynthesized α-Bi2O3 NPs, Mn-doped and Zn-doped Bi2O3 NPs against MCF-7 and HUVEC cell lines. Journal of Materials Research and Technology, 2022. 19: p. 140-150. https://doi.org/10.1016/j.jmrt.2022.05.002
4. Zare, E.N., et al., Nonspherical Metal- Based Nanoarchitectures: Synthesis and Impact of Size, Shape, and Composition on Their Biological Activity. Small, 2021. 17(17): p. 2007073. https://doi.org/10.1002/smll.202007073
5. Dhall, A. and W. Self, Cerium oxide nanoparticles: a brief review of their synthesis methods and biomedical applications. Antioxidants, 2018. 7(8): p. 97. https://doi.org/10.3390/antiox7080097
6. Arshad, R., et al., Multi-functionalized nanomaterials and nanoparticles for diagnosis and treatment of retinoblastoma. Biosensors, 2021. 11(4): p. 97. https://doi.org/10.3390/bios11040097
7. Sabir, F., et al., Onco-receptors targeting in lung cancer via application of surface-modified and hybrid nanoparticles: A cross-disciplinary review. Processes, 2021. 9(4): p. 621. https://doi.org/10.3390/pr9040621
8. Deshpande, S., et al., Size dependency variation in lattice parameter and valency states in nanocrystalline cerium oxide. Applied Physics Letters, 2005. 87(13): p. 133113. https://doi.org/10.1063/1.2061873
9. Li, M., et al., Cerium oxide caged metal chelator: anti-aggregation and anti-oxidation integrated H2O2-responsive controlled drug release for potential Alzheimer's disease treatment. Chemical Science, 2013. 4(6): p. 2536-2542. https://doi.org/10.1039/c3sc50697e
10. Mandoli, C., et al., Stem cell aligned growth induced by CeO2 nanoparticles in PLGA scaffolds with improved bioactivity for regenerative medicine. Advanced Functional Materials, 2010. 20(10): p. 1617-1624. https://doi.org/10.1002/adfm.200902363 https://doi.org/10.1002/adfm.201090042
11. Vassie, J.A., J.M. Whitelock, and M.S. Lord, Targeted delivery and redox activity of folic acid-functionalized nanoceria in tumor cells. Molecular Pharmaceutics, 2018. 15(3): p. 994-1004. https://doi.org/10.1021/acs.molpharmaceut.7b00920
12. Ivanov, V.K., A.B. Shcherbakov, and A. Usatenko, Structure-sensitive properties and biomedical applications of nanodispersed cerium dioxide. Russian chemical reviews, 2009. 78(9): p. 855. https://doi.org/10.1070/RC2009v078n09ABEH004058
13. Korsvik, C., et al., Superoxide dismutase mimetic properties exhibited by vacancy engineered ceria nanoparticles. Chemical communications, 2007(10): p. 1056-1058. https://doi.org/10.1039/b615134e
14. Celardo, I., et al., Ce3+ ions determine redox-dependent anti-apoptotic effect of cerium oxide nanoparticles. ACS nano, 2011. 5(6): p. 4537-4549. https://doi.org/10.1021/nn200126a
15. Yokel, R.A., et al., The yin: an adverse health perspective of nanoceria: uptake, distribution, accumulation, and mechanisms of its toxicity. Environmental Science: Nano, 2014. 1(5): p. 406-428. https://doi.org/10.1039/C4EN00039K
16. Varma, R.S., Greener approach to nanomaterials and their sustainable applications. Current Opinion in Chemical Engineering, 2012. 1(2): p. 123-128. https://doi.org/10.1016/j.coche.2011.12.002
17. Darroudi, M., et al., Green synthesis and evaluation of metabolic activity of starch mediated nanoceria. Ceramics International, 2014. 40(1): p. 2041-2045. https://doi.org/10.1016/j.ceramint.2013.07.116
18. Miri, A., S. Akbarpour Birjandi, and M. Sarani, Survey of cytotoxic and UV protection effects of biosynthesized cerium oxide nanoparticles. Journal of Biochemical and Molecular Toxicology, 2020. 34(6): p. e22475. https://doi.org/10.1002/jbt.22475
19. Miri, A., et al., Cerium oxide nanoparticles: green synthesis using Banana peel, cytotoxic effect, UV protection and their photocatalytic activity. Bioprocess and Biosystems Engineering, 2021. 44(9): p. 1891-1899. https://doi.org/10.1007/s00449-021-02569-9
20. Varma, R.S., Journey on greener pathways: from the use of alternate energy inputs and benign reaction media to sustainable applications of nano-catalysts in synthesis and environmental remediation. Green Chemistry, 2014. 16(4): p. 2027-2041. https://doi.org/10.1039/c3gc42640h
21. Varma, R.S., Greener routes to organics and nanomaterials: sustainable applications of nanocatalysts. Pure and Applied Chemistry, 2013. 85(8): p. 1703-1710. https://doi.org/10.1351/PAC-CON-13-01-15
22. Hamidian, K., et al., Photocatalytic performance on degradation of Acid Orange 7 dye using biosynthesized un-doped and Co doped CeO2 nanoparticles. Materials Research Bulletin, 2021. 138: p. 111206. https://doi.org/10.1016/j.materresbull.2021.111206
23. Hamidian, K., et al., Doped and un-doped cerium oxide nanoparticles: Biosynthesis, characterization, and cytotoxic study. Ceramics International, 2021. 47(10): p. 13895-13902.

https://doi.org/10.1016/j.ceramint.2021.01.256
24. Miri, A., M. Sarani, and M. Khatami, Correction: Nickel-doped cerium oxide nanoparticles: biosynthesis, cytotoxicity and UV protection studies. Rsc Advances, 2020. 10(11): p. 6735-6735. https://doi.org/10.1039/D0RA90014A
25. Miri, A., et al., Using biebersteinia multifida aqueous extract, the photocatalytic activity of synthesized silver nanoparticles. Oriental Journal of Chemistry, 2018. 34(3): p. 1513. https://doi.org/10.13005/ojc/340342
26. Fernandes, V., et al., Room temperature ferromagnetism in Co-doped Ce O 2 films on Si (001). Physical Review B, 2007. 75(12): p. 121304. https://doi.org/10.1103/PhysRevB.75.121304
27. Ahamed, M., et al., Green synthesis, characterization and evaluation of biocompatibility of silver nanoparticles. Physica E: Low-dimensional Systems and Nanostructures, 2011. 43(6): p. 1266-1271. https://doi.org/10.1016/j.physe.2011.02.014
28. Mukherjee, P., et al., Bioreduction of AuCl4– ions by the fungus, Verticillium sp. and surface trapping of the gold nanoparticles formed. Angewandte Chemie International Edition, 2001. 40(19): p. 3585-3588. https://doi.org/10.1002/1521-3773(20011001)40:19<3585::AID-ANIE3585>3.0.CO;2-K
29. Von White, G., et al., Green synthesis of robust, biocompatible silver nanoparticles using garlic extract. Journal of nanomaterials, 2012. 2012. https://doi.org/10.1155/2012/730746
30. Irshad, M.S., et al., Green synthesis, cytotoxicity, antioxidant and photocatalytic activity of CeO2 nanoparticles mediated via orange peel extract (OPE). Materials Research Express, 2019. 6(9): p. 0950a4. https://doi.org/10.1088/2053-1591/ab3326
31. Rajan, A.R., et al., Synthesis of nanostructured CeO2 by chemical and biogenic methods: optical properties and bioactivity. Ceramics International, 2020. 46(9): p. 14048-14055. https://doi.org/10.1016/j.ceramint.2020.02.204